HMG Advance Access published August 15, 2016

HDAC inhibition in the *cpfl1* mouse protects degenerating cone photoreceptors *in vivo*

Dragana Trifunović[1*#], Blanca Arango-Gonzalez[1#], Antonella Comitato[2], Melanie Barth[1], Eva M. del Amo[3], Manoj Kulkarni[1], Ayse Sahaboglu[1], Stefanie M. Hauck[4], Arto Urtti[3,5], Yvan Arsenijevic[6], Marius Ueffing[1], Valeria Marigo[2], François Paquet-Durand[1]

Affiliations

[1]Institute for Ophthalmic Research, University of Tuebingen, 72076 Tuebingen, Germany

[2]Department of Life Sciences, University of Modena and Reggio Emilia, 41125 Modena, Italy

[3]School of Pharmacy, University of Eastern Finland, 70211 Kuopio, Finland

[4]Research Unit Protein Science, Helmholtz Center Munich, 85764 Neuherberg, Germany

[5]Centre for Drug Research, Division of Pharmaceutical Bioscience, University of Helsinki, 00014 Helsinki, Finland

[6]Unit of Gene Therapy & Stem Cell Biology, Hôpital Ophtalmique Jules Gonin, 1004 Lausanne, Switzerland

[#]These authors contributed equally to this work

[*]Correspondence should be sent to:

Dragana Trifunović

Institute for Ophthalmic Research

University of Tuebingen

Roentgenweg 11, 72076 Tuebingen, Germany

e-mail: dragana.trifunovic@uni-tuebingen.de

phone: +49 (0) 7071 29 80741

Fax: +49 (0) 7071 29 5777

Abstract

Cone photoreceptor cell death as it occurs in certain hereditary retinal diseases is devastating, with the affected patients suffering from a loss of accurate and color vision. Regrettably, these hereditary cone diseases are still untreatable to date. Thus, the identification of substances able to block or restrain cone cell death is of primary importance. We studied the neuroprotective effects of a histone deacetylase inhibitor, Trichostatin A (TSA), in a mouse model of inherited, primary cone degeneration (*cpfl1*). We show that HDAC inhibition protects *cpfl1* cones *in vitro*, in retinal explant cultures. More importantly, *in vivo*, a single intravitreal TSA injection significantly increased cone survival for up to 16 days post-injection. In addition, the abnormal, incomplete cone migration pattern in the *cpfl1* retina was significantly improved by HDAC inhibition. These findings suggest a crucial role for HDAC activity in primary cone degeneration and highlight a new avenue for future therapy developments for cone dystrophies and retinal diseases associated with impaired cone migration.

Introduction

Cone photoreceptors in the human retina are responsible for sharp high resolution vision and color discrimination. Hereditary cone degenerations, such as in Stargardt´s and Best´s disease, achromatopsia, and cone dystrophies are caused by mutations in single genes, and lead to severe visual impairment, reduced visual acuity and loss of color vision. Cone dystrophies are characterized by a high genetic heterogeneity, with disease causing mutations in at least 27 genes (RetNet: https://sph.uth.edu/retnet). In addition, a genetic contribution has also been proposed for complex diseases affecting cones, such as in age-related-macular degeneration (AMD) or diabetic retinopathy (DR). Irrespective of the genetic cause, a common outcome of retinal diseases is neuronal cell death, giving a strong rationale for targeted neuroprotective approaches that may prevent or delay cell death execution (1).

The c*one photoreceptor function loss-1* (*cpfl1*) mutant mouse is an animal model for autosomal recessive achromatopsia or progressive cone dystrophy (2). This model is unique in the sense that it is characterized by an early onset of cone loss at post-natal day 14 (PN14) and a fast progression with the peak of cell death at PN24 (3). We have previously shown that photoreceptor cell death in the *cpfl1* mouse, as well as in nine other animal models for inherited retinal degeneration, follows a non-apoptotic mechanism, characterized by accumulation of cGMP, increased activities of cGMP-dependent protein kinase (PKG), histone deacetylase (HDAC), poly-ADP-ribose-polymerase (PARP), and calpain proteases, as well as accumulation of poly-ADP-ribose (PAR) (4, 5). In addition, the *cpfl1* cone degeneration is also associated with prominent defects in cone migration (3).

A common non-apoptotic cell death mechanism in different retinal degeneration models provides a rationale for the identification of therapeutic targets that would prove beneficial for a broader population of patients suffering from a variety of different genetic causes (4, 6). While, numerous attempts to restrain the execution of rod photoreceptor cell death were described (6-11) to date, an effective clinical treatment for primary cone photoreceptor degeneration has not been reported. Since humans use mostly cones for

their vision, a development of treatment protocols to preserve cones is of highest priority in clinical ophthalmology.

The interplay between histone acetylation and deacetylation, performed by histone acetyltransferases (HATs) and histone deacetylases (HDACs) respectively, determines the transcription state of genes in general (12), and this is also true for photoreceptor-specific genes (13, 14). Aberrant activity of histone deacetylases is associated with a number of diseases with very different etiology, ranging from cancer to neurodegenerative diseases (15). Consequently, in current medicine, HDAC inhibition is discussed as one of the most promising novel therapeutic approaches for various diseases (16).

In the present study, we tested the hypothesis that hereditary cone degeneration can be prevented or delayed by HDAC pharmacological inhibition. We assessed cone photoreceptor survival after HDAC inhibition with Trichostatin A (TSA) *in vitro*, on retinal explant cultures obtained from *cpfl1* animals, as well as *in vivo*, after intravitreal injection. We show that TSA protects *cpfl1* cones both *in vitro* and *in vivo*. Importantly, a single TSA injection *in vivo* achieved a significant protection of cone photoreceptors, up to sixteen days post-injection. In addition, we observed a significant improvement of impaired cone migration, present in the degenerating *cpfl1* retina. Our study highlights the possibility to use pharmacological HDAC inhibition for substantial cone protection in an inherited cone dystrophy, and may forward the future development of therapies aimed at cone photoreceptor preservation.

Results

HDAC activity is increased in *cpfl1* photoreceptors

We have previously shown that the *cpfl1* cone photoreceptor degeneration follows a non-apoptotic cell death mechanism characterized by increased HDAC activity at the peak of degeneration at PN24 (4). In this study, we evaluated HDAC activity also at the onset of cone degeneration (PN14) and found significantly more HDAC activity positive photoreceptors in mutant retinas compared to wild-type (wt) (Supplementary material Fig. S1A-F). Increased HDAC activity present also at PN24 was significantly decreased after the TSA treatment ($p=0.004$; Supplementary material Fig. S1G).

HDAC inhibition with TSA rescues degenerating cones *in vitro*

To test whether HDAC inhibition could promote cone photoreceptor survival, we used *cpfl1* long-term retinal explants cultured under entirely defined conditions, in serum-free medium. Both *cpfl1* and wt retinas were explanted at the onset of *cpfl1* degeneration (PN14) and cultured for 2 days in regular R16 retinal culture medium, without any treatment. Retinas were then exposed to 10 nM TSA every second day, until PN24. In the untreated *cpfl1* explants almost half of the cones were lost at PN24, as assessed by the percentage of cones in the outer nuclear layer (ONL), identified by labeling with an antibody for glycogen phosphorylase (Glyphos) (17). When compared to untreated wt explants (n=4), only ~53% of cones are still present in *cpfl1* retina as shown in Figure 1 (52.91% ± 7.18 SEM, n=7). Treatment with 10 nM TSA increased the percentage of surviving cones in *cpfl1* explants to wt levels (109.76% ± 10.34, n=6, $p= 0.0023$), indicating near complete cone protection. On the other hand, TSA had no significant effect on cone photoreceptors in wt cultures (110.27% ± 23.18 SEM, n=3).

Intravitreal TSA injection protects degenerating cones *in vivo*

These promising *in vitro* results prompted us to further evaluate the protective effects of HDAC inhibition *in vivo*. To guide and optimize the *in vivo* treatment scheme, we first tried to predict the potential half-life of the drug inside the eye. Model calculations suggested that intravitreal clearance of TSA in the rabbit eye was 0.478 ml/h, and the half-life was in the range of 1.7-3.3 hours. In the mouse, the calculated intravitreal half-life of TSA was an order of magnitude shorter (about 17 minutes), and more than 90% of the dose was expected to be eliminated in one hour after injection (Supplementary material Fig. S2 and Note 1).

Since our *in vitro* experiments suggested that 10 nM TSA was efficiently protecting cones, we wanted to test if the same concentration would be effective also *in vivo*. As controls, we included both non-treated and sham treated eyes in the analysis. At PN14, nine animals from three different litters received an injection of 0.5 µl of a 100 nM TSA solution in one eye, with an estimated final TSA concentration of 10 nM. The contralateral eyes were sham injected with vehicle to control for injection-specific effects. Mice

were sacrificed and analyzed 10 days later, at PN24. Consistent with our *in vitro* results, TSA significantly increased the percentage of surviving cones in treated *vs*. sham treated eyes (*cpfl1* sham: 84.92% ± 3.1 SEM, n=9; *cpfl1* treated: 99.88% ± 4.83, n=9, *p=0.026*; Fig. 2). The percentage of cones in sham injected eyes was comparable to the percentage of cones in non-treated *cpfl1* mice (*cpfl1*: 78.24% ± 2.53 SEM, n=8; *cpfl1* sham: 84.92% ± 3.1, n=9), suggesting that the injection itself had no effect on cone survival. The number of cones in sham- or 10 nM TSA- treated wt retinas were similar to non-treated wt retinas confirming the *in vitro* observation that TSA in the studied dosage had no deleterious effect on healthy cones (wt sham: 102.37% ± 4.72, n=8; wt treated: 106.11% ± 7.02, n=8, Fig. 2). The *in vivo* results suggested a remarkable protection of degenerating cones by a single intravitreal injection of 10 nM TSA with the number of cones in treated retinas reaching 99.8% of wt levels. To then test if TSA could efficiently protect degenerating cones at even lower concentrations, we performed a single intravitreal injection of TSA with a final estimated concentration of 1 nM, at PN14, and evaluated the protective effects at PN24. Remarkably, 1 nM TSA single treatment yielded a protective effect comparable to the 10 nM dose (Fig. 2, *cpfl1* sham: 83.24% ± 2.92 SEM, n=10; *cpfl1* treated: 98.3% ± 5.25, n=11, *p=0.03*).

To assess protective effect of HDAC inhibition at longer time points, we treated the *cpfl1* animals with a single intravitreal injection of 10 nM TSA and assessed cone survival at PN30, *i.e.* after the peak of degeneration. When compared to untreated PN30 wt retina, cone loss in sham-treated *cpfl1* had progressed further, with 71.6% ± 3.77 cones remaining (Fig. 3). In contrast, in 10 nM TSA treated eyes, even 16 days after a single intravitreal injection, the percentage of cones was significantly higher than in sham-treated, with 88.74% ± 2.79 cones still present (n=5, *p=0.007*). However, the protective effect at PN30 was less pronounced than at PN24, with the number of surviving cones lower than in wt retina (*p=0.03*).

To understand whether the observed increase in the cone numbers after TSA treatment was due to an indirect effect of a reduced clearance by microglia, we assessed the status of microglia using a staining against ionized-calcium-binding-adapter molecule 1 (IBA1) (18). Although activated microglia appeared to be present to some extent in the different layers of the retina, we neither detected a microglial invasion

of the ONL, nor differences in IBA1 positive cells, with or without TSA treatment (Supplementary material Fig. S3). Alternatively, the protective effect of TSA might have been related to a delay of cone maturation in *cpfl1* animals. To address this possibility, we also characterized the status of cone differentiation by looking at the expression and localization of M- and S-opsins, as well as cone-specific transducin (GNAT2), previously reported to be abnormally distributed in degenerating cones (19). Although M-opsin was seen in untreated cone outer segments, *cpfl1* cones frequently showed opsin mislocalization to the cell body (Fig. 4G, arrows) and synaptic terminals (Fig. 4G, arrowheads). S-opsin staining revealed short outer segments as well as opsin mislocalization (Fig. 4H, arrows) in untreated *cpfl1* cones and a similar but more pronounced mislocalization was observed for GNAT2 (Fig. 4I, arrows). In contrast, double staining for M- and S-opsin with Glyphos indicated that cones protected by TSA had normal morphology, with clearly developed inner and outer segments (Fig. 4J-L and P-R). In addition, the correctly positioned cones in the upper part of the ONL show both M- and S-opsin properly localized in their outer segments (Fig. 4J and R). Similarly, in surviving cones GNAT2 was properly localized in outer segments. The correct localization of cone opsins and cone transducin suggested that TSA-mediated cone preservation had no obvious adverse effects on cone development and maturation.

HDAC inhibition significantly improves impaired cone migration

We previously reported that *cpfl1* retina is characterized by impaired migration of developing cones (3). Glyphos staining of cones in degenerating *cpfl1* retina confirmed such aberrant cone positioning, both *in vitro* and *in vivo* (Fig. 5). Importantly, we observed an improved migration of cones after both *in vitro* and *in vivo* TSA treatments of retinas (Fig. 5). To evaluate the extent of the cone migration improvement, we measured the distance of the center of individual cone nuclei from the outer plexiform layer (OPL, Fig. 5, dashed red lines), which demarcates the lower boundary of the photoreceptor area. The percentage of cone migration distance from the OPL is presented in relative terms to the thickness of the ONL. In the *in vitro* situation, at PN24, wt cones migrated approximately to 70% of ONL thickness (wt untreated: 69.25% ± 2.3 SEM, n=3; wt treated: 72.66% ± 5.1, n=3), while in non-treated *cpfl1* retinas they reached

only 55%. After treatment with 10 nM TSA of *cpfl1* retinas in explant cultures, cone nuclei reached a position very similar to that of wt cones (*cpfl1* untreated: 55.31% ± 3.1 SEM, n=6; *cpfl1* treated: 65.95% ± 2.8, *p=0.029*). Similarly, cone migration was also improved in *cpfl1* retinas *in vivo*, after treatment with 1 nM TSA. Here, cones were localized significantly more distant from the outer plexiform layer (*cpfl1* untreated: 71.68% ± 1.09 SEM, n=10, *cpfl1* treated: 77.18% ± 0.84, n=11, *p=0.02*). Comparable results were obtained after treatment with 10 nM TSA (*cpfl1* untreated: 67.47% ± 1.92 SEM, n=9, *cpfl1* treated: 76.38% ± 0.73, n=9, *p=0.0005*). We did not observe changes in cone localization in wt retinas after TSA treatment (wt untreated: 86.89% ± 0.26 SEM, n=7; wt treated: 85.49% ± 0.23, n=7). Nevertheless, even though TSA treatment significantly improved *cpfl1* cone migration, cone positioning was still significantly different compared to wt cones (*cpfl1* 1 nM TSA: 77.18% ± 0.84 SEM *vs.* wt untreated: 86.89% ± 0.26, *p=0.0002*; *cpfl1* 10nM: 76.38% ± 0.73 *vs.* wt untreated: 86.89% ± 0.26, *p=0.0004*).

We previously found high cGMP accumulation and increased activity of cGMP-dependent protein kinase G (PKG) to be associated with *cpfl1* cone phenotypes (3). To investigate whether HDAC inhibition had an effect on cGMP and PKG activity after ten days of treatment with TSA, we looked for cGMP accumulation and the phosphorylation status of a well-known PKG substrate, vasodilator-stimulated-protein (pVASP) (20), with and without TSA treatment. Untreated *cpfl1* retinas showed cGMP accumulation in cone segments as well as in cone cell bodies (as evidenced by Glyphos co-labeling). There were no obvious differences in cone cGMP accumulation after TSA treatment. (Supplementary material Fig. S4A). Likewise, some cones, visualized by Glyphos staining, were also positive for pVASP in both TSA treated and untreated *cpfl1* retinas, with no evident differences between the two (Fig. S4B). Taken together, these results indicated that HDAC activity (and TSA inhibition) operated down-stream of the mutation-induced cGMP accumulation.

Discussion

Hereditary diseases of cone photoreceptors are currently untreatable and lead to major visual impairment and blindness. Our study in the *cpfl1* mouse model demonstrates prominent cone protection after HDAC inhibition, *in vitro* and *in vivo,* and thus confirms that HDAC activity is causally involved in hereditary cone photoreceptor degeneration. This provides a proof-of-principle for the further development of HDAC inhibition as a novel therapeutic approach for cone dystrophies.

HDAC inhibition was found to induce cell death in tumor cells derived from various cancers (21), while in neurodegenerative diseases, the same treatment may prolong cell survival (22). In the retina, HDAC inhibitors have been discussed as a potential therapeutic strategy for ischemic retinal injury, with different HDAC inhibitors affording structural and functional neuroprotection after experimental ischemia (23). Furthermore, HDAC inhibition was shown to slow rod photoreceptor degeneration in an animal model for Retinitis Pigmentosa (24). Importantly, current clinical trials are suggesting beneficial effects of treatments with a HDAC inhibitor in patients suffering from Retinitis Pigmentosa (25, 26). We show here for the first time that HDAC inhibition significantly protects cones in a mouse model for hereditary cone dystrophy. Besides its implication for future treatment of rare forms of retinal degeneration, the results presented here may also extend to common diseases of the retina, including DR and AMD, where cone degeneration is the cause of legal blindness.

An important result from our study is that a single intraocular application significantly protected *cpfl1* cones for at least two weeks post-injection. This is unexpected, as our calculations on TSA clearance suggested that the drug was below threshold concentration, after less than 2 hours and may point to an imprinting mechanism, beyond the transient presence of TSA. This is in line with previous studies which found that TSA leads to robust protein acetylation after 3 hours (13) or to transcriptional changes after only 5 minutes (27), supporting the possibility of epigenetic mechanisms. The molecular mechanism underlying treatments with HDAC inhibitors are still not well characterized. In *cpfl1* retina, a previous study found an upregulation of STAT3 signaling which was suggested as an endogenous neuroprotective response (28). Interestingly, STAT3 activation may be controlled by HDAC activity (29).

Importantly, the TSA clearance estimation suggested that cone degeneration was halted already after a short-time intraocular exposure. This observation could be especially relevant for patients with retinal dystrophies where monthly intravitreal injections are usually well tolerated (30). Since in mice the protective effect was present for at least 10 days post-injection, a rough extrapolation from mouse to man, would suggest that in humans an intravitreal dosing once per three months might be sufficient (31). Alternatively, formulations for local application to the eye would minimize the potential side-effects observed in some cases of long-term, systemic HDAC inhibition (26, 32, 33).

Cone photoreceptor development is characterized by a migration within the ONL, from the outer limiting membrane inwards to the OPL, and then outwards, until they reach their final position just below the outer limiting membrane, from PN12 onwards (34). Cone degeneration in mouse models is characterized not only by cone loss, but also by improper developmental cone migration (3, 35). In fact, delayed cone migration was also reported in mouse models with rod degeneration as an indirect consequence of rod cell death (34). Migration of cone photoreceptors also occurs in human retinal development, where in the fovea cones are migrating laterally towards the foveal pit (36). Cone misplacement has been associated with human retinal diseases of different etiology as improper cone migration can lead to foveal hypoplasia (37). This is observed, for instance, in patients suffering from albinism (38), idiopathic congenital nystagmus (37), and also from achromatopsia (39). In addition, cone misplacement was reported in aged patients suffering from AMD (40). We found that TSA treatment not only prevented cone degeneration but also significantly improved aberrant cone migration in degenerating *cpfl1* retina. There are numerous reports on the effects of HDAC inhibition on cell migration. The effects of HDAC inhibition on improved cell migration could take place via inhibition of the cytoplasmic histone deacetylase (HDAC6) resulting in higher acetylation of α-tubulin necessary for stability of microtubules in migrating cells (41). Alternatively, HDAC inhibition could lead to epigenetic changes governing migration of photoreceptors, a process still not fully understood. TSA treatment significantly improved the migration of misplaced *cpfl1* cones both *in vitro* and *in vivo*. Nevertheless, HDAC inhibition alone was not sufficient to fully repair the cone migration defect in *cpfl1* retinas. A plausible explanation could

relate to increased PKG activity in *cpfl1* retina, as we previously reported (3). PKG-specific phosphorylation of the serine 239 residue of VASP was shown to negatively regulate neuronal migration (42). Proteins of the Ena/VASP family are regulators of actin assembly and cell motility as they are localized in focal adhesions (43). cGMP-dependent PKG overactivation leads to VASP phosphorylation, which will result in removal of VASP from focal adhesions, contributing to altered cell migration (44). Our data suggest that TSA inhibition of HDACs did not reduce VASP phosphorylation of serine 239 as assessed by immunostaining. The possible dual regulation of cone photoreceptor migration, one via PKG overactivation and the other involving aberrant HDAC activity, will require further specific studies. In addition, in the *cpfl1* mouse model, the mutation-induced loss of cone photoreceptors coincides in part with postnatal retinal development (3, 45). As the TSA treatment during the third postnatal week overlaps in time with the establishment of retinal connectivity (46), further studies (*i.e.* rod ERG analysis) are also necessary to define how restoration of the normal developmental cone migration pattern under the influence of HDAC inhibitors may alter rod connectivity and function.

Degenerating cones in *cpfl1* retina are characterized by cGMP accumulation as a consequence of the non-functional cone photoreceptor PDE6 enzyme (3, 4). We did not observe obvious changes in the numbers of cells showing cGMP accumulation after the treatment, indicating that TSA-driven protection of cones probably operates down-stream in the degenerative pathway. Increasing lines of evidence suggest PKG as one of the main initiators of a photoreceptor cell death cascade (4, 6, 47). Previously, we found that increased PKG and HDAC activities were temporally connected in 10 different animal models for inherited retinal degeneration (4). This corresponds to observations in *C. elegans* where PKG activity was found to regulate HDAC activation (48). Since HDAC inhibition did not seem to affect VASP phosphorylation in cones, our study indicates that during cell death HDAC activity may occur independently of- or downstream of PKG. The underlying mechanisms through which HDAC inhibition offers cone protection remains to be determined.

HDAC activity is also crucial for mouse photoreceptor development as HDAC inhibition at early post-natal retinal development (PN2) leads to a complete loss of developing rod photoreceptors (49). In the

mouse retina cone photoreceptors are born prenatally (45), therefore we do not expect an effect of TSA on cone birth, but the full maturation and commitment towards blue cones (S cones) or red/green cones (M cones) takes place during the second postnatal week (50). Since we performed HDAC inhibition just after this time-period, we assessed the expression and localization of S- and M-opsin, to address whether the observed increase in cone survival following HDAC inhibition was due to cone development and maturation delays. In addition, we checked for the cone specific transducin (GNAT2), a member of the cone phototransduction cascade (51). The observed correct localization of cone opsins and transducin suggests that late postnatal HDAC inhibition did not affect cone cell development and maturation. However, we cannot exclude the possibility that the rapid degeneration of *cpfl1* cones was in part caused by developmental defects. In this case TSA treatment, in a critical time-frame, may have supported normal development as the observed effects lasted for more than two weeks. Future studies, for instance on more slowly progressing cone degeneration models, may reveal whether TSA and HDAC inhibition mediated cone protection can be applied to cone degeneration in general, irrespective of developmental stage and disease pathogenesis.

In summary, this study is the first to show that HDAC inhibition can significantly delay cone loss in a mouse model for a human cone dystrophy. While the effect of TSA on *cpfl1* retina *in vivo* lasts until at least one month post-natal, further studies will be needed to determine the duration of the protection and to establish long-term treatment paradigms. Remarkably, HDAC inhibition appeared to have a dual effect on both cone survival and cone migration without obvious effects on cone differentiation and development. Our study thus provides a proof-of-principle for the potential of HDAC inhibitors as therapeutic agents for cone photoreceptor protection. Importantly, this may be applicable not only to hereditary cone dystrophies, but possibly also to common retinal diseases associated with cone degeneration such as diabetic retinopathy (52, 53), as well to diseases where cone degeneration is accompanied by improper cone migration, such as age-related macular degeneration (40).

Materials and Methods

Animals

Cpfl1 and congenic C57BL/6 wild-type (wt) animals were housed under standard white cyclic lighting, had free access to food and water, and were used irrespective of gender. All procedures were approved by the Tübingen University committee on animal protection (Einrichtung für Tierschutz, Tierärztlichen Dienst und Labortierkunde) and performed in accordance with the ARVO statement for the use of animals in ophthalmic and visual research. Procedures performed at the polistab of University of Modena and Reggio Emilia (*in vivo* treatment on *cpfl1* and wt animals) were reviewed and approved by the local ethical committee (Prot. N. 50 12/03/2010). All efforts were made to minimize the number of animals used and their suffering.

Immunofluorescence

Retinae were fixed in 4% paraformaldehyde (PFA) in 0.1 M phosphate buffer (pH 7.4) for 45 min at 4°C. Sagittal 12 µm sections were collected, air-dried and stored at -20°C. Sections were incubated overnight at 4°C with primary antibodies. The primary antibodies used were specific for Glycogen phosphorylase (Glyphos, 1:1000 dilution, kindly provided by Prof. Pfeiffer-Guglielmi (17)), cone arrestin (1:1000, AB15282, Millipore, Darmstadt, Germany), IBA1 (1:200, 019-19741, Wako, Richmond, USA), M-opsin (1:200, AB5405, Millipore), S-opsin (1:200, AB5407, Millipore), GNAT2 (1:200, sc-390, Santa Cruz, Dallas, USA), cGMP (1:500, kindly provided by Prof. Steinbusch, University of Maastricht, The Netherlands (54)) and phospho-VASP (Ser239) (1:200 dilution, 0047-100/VASP-16C2, Nanotools, Teningen, Germany (3, 44)). Alexa Fluor 488- or 566-conjugated were used as secondary antibodies (Molecular Probes, Inc. Eugene, USA). Negative controls were carried out by omitting the primary antibody. Specificity of cone labeling with Glyphos was shown by co-labelling with peanut-agglutinin (Supplementary Fig. S5), a well-established marker for cones (55).

HDAC *in situ* activity assay

HDAC activity assays were performed on cryosections of 4% PFA- fixed eyes. The assay is based on an adaptation of the Fluor de Lys Fluorescent Assay System (Biomol, Hamburg, Germany). Retina sections were exposed to 200 µM Fluor de Lys-SIRT2 deacetylase substrate (Biomol) with 500 µM NAD+ (Biomol) in assay buffer (50 mM Tris/HCl, 137 mM NaCl; 2.7 mM KCl; 1 mM MgCl2; pH 8.0) for 3 hours at room temperature (8). Sections were then washed in PBS and fixed in methanol at -20°C for 20 min. Slides were mounted with developer (Biomol; KI105, diluted 1:20 in assay buffer) containing 2 µM TSA (Sigma, Steinheim, Germany) and 2 mM NAM (Sigma). Negative controls consisted of omitting the substrate (Supplementary Fig.S1E).

Retinal explant cultures

Organotypic retinal cultures from *cpfl1* (n=7) and wt (n=4) animals that included the retinal pigment epithelium (RPE) were prepared under sterile conditions. Briefly, PN14 animals were sacrificed, the eyes enucleated and pretreated with 0.12% proteinase K (ICN Biomedicals Inc., OH, USA) for 15 minutes at 37°C in R16 serum free culture medium (Order No.: 074-90743A; Gibco, Paisley, UK). Proteinase K activity was blocked by addition of 10% fetal bovine serum, followed by rinsing in serum-free medium. Following this, the cornea, lens, sclera and choroid were removed carefully, with only the RPE remaining attached to the retina. The explant was then cut into four wedges, to give a clover-leaf like structure, which was transferred to a culture membrane insert (Corning Life Sciences, Lowell, USA) with the RPE facing the membrane. The membrane inserts were placed into six well culture plates with R16 medium (Gibco, Paisley, UK) and incubated at 37°C in a humidified 5% CO_2 incubator. The culture medium was changed every 2 days during the 10 culturing days.

Retinal explants were left without treatment for 2 days (until PN16), followed by 10 nM Trichostatin A (TSA) treatment (≥98% (HPLC), from Streptomyces sp., Sigma-Aldrich, St-Louis, USA). TSA was dissolved in 0.2% dimethyl sulfoxide (DMSO; Sigma) and diluted in R16 culture medium. For controls, the same amount of DMSO was diluted in culture medium. Culturing was stopped at PN24 by 2 h fixation

in 4% PFA, cryoprotected with graded sucrose solutions containing 10, 20, and 30% sucrose and then embedded in tissue freezing medium (Leica Microsystems Nussloch GmbH, Nussloch, Germany).

In vivo injections

Animals were anesthetized with an intraperitoneal injection of Avertin (250 mg/kg) (1.25% (w/v) 2,2,2-tribromoethanol and 2.5% (v/v) 2-methyl-2-butanol; Sigma, Milan, IT) and kept warm during injections. Single intravitreal injections were performed at PN14 on one eye while the other eye was sham injected with 0.0001% DMSO (in 0.9% NaCl solution) as contralateral control. TSA (1 and 10 nM) was diluted in 0.9% NaCl solution. Injections were performed with 0.5 µl of 10 nM and 100 nM TSA in order to have a final concentration of 1 nM and 10 nM, respectively, assuming the free intraocular volume of mouse eye to be 5µl (http://prometheus.med.utah.edu/~marclab/protocols.html). Eleven *cpfl1* animals and eight wt from three different litters were used for intravitreal injections and were sacrificed 10 days after treatment (PN24). For the treatment of *cpfl1* animals until PN30 injections were performed at PN14 in five different animals with one eye being injected with 10 nM TSA, while the other eye was sham injected. Eyes were immediately enucleated, fixed for 2 h in 4% PFA and prepared for cryosectioning (see 'Retinal explant cultures'). Sections were labeled in a non-conclusive fashion to allow for an investigator-blind analysis.

Microscopy, cell counting, and statistical analysis

Fluorescence microscopy was performed on an Axio Imager Z1 ApoTome Microscope, equipped with a Zeiss Axiocam MRm digital camera. Images were captured using Zeiss Axiovision 4.7 software. Adobe Photoshop CS3 (Adobe Systems Incorporated, San Jose, CA, USA) was used for primary image processing. Quantifications were performed on pictures captured on at least nine different random positions of at least three sagittal sections for at least four different animals for each genotype and treatment using Z-stacks mode of Axiovision 4.7 at 20x magnification. The average area occupied by a photoreceptor cell (*i.e.* cell size) for each individual eye was determined by counting DAPI-stained nuclei

in nine different areas (50 x 50 µm) of the retina. The total number of photoreceptor cells was estimated by dividing the outer nuclear layer (ONL) area by this average cell size. The quantification of cones was performed by manually counting the number of positively labelled cones in the ONL. Values obtained are given as fraction of total cell number in ONL (*i.e.* as percentage) and normalized to the wt situation. Values are expressed as average ± standard error of the mean (SEM). For statistical comparisons the two-tailed, unpaired Student t-test as implemented in Prism 6 for Windows (GraphPad Software, La Jolla, CA, USA) was employed.

To assess differences in cone migration, the distance in µm between the outer plexiform layer (OPL) and the center of Glyphos positive cell bodies was measured using Axiovision software (Zeiss). Distance values for 150-250 cones in the entire retinas were averaged on Glyphos immunostained sections from at least 5 different animals for each genotype. The migration profile of cones was presented as the relative migration distance to ONL thickness measured using Axiovision software. Statistical differences between experimental groups were calculated using Student's two-tailed, unpaired t-test and Microsoft Excel software (Microsoft, Seattle, WA, USA). Error bars in the figures indicate SEM, levels of significance were: * = $p<0.05$, ** = $p<0.01$, *** = $p<0.001$.

Assessment of intravitreal clearance of TSA

The intravitreal clearance (CL_{ivt}) of TSA was calculated *in silico* using the Quantitative structure-property relationships (QSPR) model published recently (56) based on comprehensive rabbit data from intravitreal injection experiments: $LogCL_{ivt}$= -0.25269 - 0.53747 (LogHD) + 0.05189 ($LogD_{7.4}$), where HD is the number of hydrogen bond donor atoms and $LogD_{7.4}$ is the calculated n-octanol/water distribution coefficient at pH 7.4 of the compound. The model is built based on small molecular weight compounds using the linear multivariate analysis tools: principal component analysis (PCA) and linear partial least square (PLS) (Simca Plus, version 10.5, Umetrics AB, Umea, Sweden). Firstly, the chemical structure of the TSA was retrieved from ACD/Dictionary from ACDlabs software (version 12, Advanced Chemistry Development, Inc., Toronto, Canada) and was used as input in ACDlabs software to generate

30 molecular descriptors: pK_a for the most acidic molecular form, pK_a for the most basic form, LogD at pH 5.5 and 7.4, LogP, MW, PSA (polar surface area), FRB (freely rotatable bonds), HD (hydrogen bond donors), HA (hydrogen bond acceptors), Htot (HD + HA), rule of 5, molar refractivity, molar volume, parachor, index of refraction, surface tension, density, polarizability, C ratio, N ratio, NO ratio, hetero ratio, halogen ratio, number of rings and number of aromatic, 3-, 4-, 5- and 6-membered rings. The applicability domain of the intravitreal clearance model for TSA was inspected generating the PCA score plot of the training set of the model together with TSA (Supplementary Fig. S2). Compounds that lie inside the ellipse depicted in the plot belong to the same chemical space of the model and are predictable by the model. Once the applicability domain was confirmed, the intravitreal clearance value of TSA was calculated with the above equation using the descriptors values (LogD at pH 7.4 and HD). Half-life was calculated using equation $t_{1/2} = \ln 2\ V_d/CL$, where V_d is the volume of distribution and CL is the intravitreal clearance. For a brief discussion on the transferability between rabbit and mouse data, see supplementary note 1.

Acknowledgements

We are grateful to Prof. E. Zrenner for fruitful discussions and support, we also thank K. Masarini and N. Rieger for skillful technical assistance, and M. Power for critically reading of the manuscript. This work was supported by the Kerstan Foundation, Deutsche Forschungsgemeinschaft [DFG TR 1238/4-1, DFG PA1751/4-1], Alcon Research Institute, European Commission [DRUGSFORD: HEALTH-F2-2012-304963], German Ministry of Education and Research [BMBF HOPE2 – FKZ 01GM1108A].

Competing financial interests

The authors declare no competing financial interests.

References

1 Trifunovic, D., Sahaboglu, A., Kaur, J., Mencl, S., Zrenner, E., Ueffing, M., Arango-Gonzalez, B. and Paquet-Durand, F. (2012) Neuroprotective strategies for the treatment of inherited photoreceptor degeneration. *Curr. Mol. Med.*, **12**, 598-612.

2 Thiadens, A.A., den Hollander, A.I., Roosing, S., Nabuurs, S.B., Zekveld-Vroon, R.C., Collin, R.W., De Baere, E., Koenekoop, R.K., van Schooneveld, M.J., Strom, T.M. *et al.* (2009) Homozygosity mapping reveals PDE6C mutations in patients with early-onset cone photoreceptor disorders. *Am. J. Hum. Genet.*, **85**, 240-247.

3 Trifunovic, D., Dengler, K., Michalakis, S., Zrenner, E., Wissinger, B. and Paquet-Durand, F. (2010) cGMP-dependent cone photoreceptor degeneration in the cpfl1 mouse retina. *J. Comp. Neurol.*, **518**, 3604-3617.

4 Arango-Gonzalez, B., Trifunovic, D., Sahaboglu, A., Kranz, K., Michalakis, S., Farinelli, P., Koch, S., Koch, F., Cottet, S., Janssen-Bienhold, U. *et al.* (2014) Identification of a common non-apoptotic cell death mechanism in hereditary retinal degeneration. *PloS One*, **9**, e112142.

5 Kulkarni, M., Trifunovic, D., Schubert, T., Euler, T. and Paquet-Durand, F. (2016) Calcium dynamics change in degenerating cone photoreceptors. *Hum. Mol. Genet.*, in press.

6 Paquet-Durand, F., Hauck, S.M., van Veen, T., Ueffing, M. and Ekstrom, P. (2009) PKG activity causes photoreceptor cell death in two retinitis pigmentosa models. *J. Neurochem.*, **108**, 796-810.

7 Sahaboglu, A., Tanimoto, N., Kaur, J., Sancho-Pelluz, J., Huber, G., Fahl, E., Arango-Gonzalez, B., Zrenner, E., Ekstrom, P., Lowenheim, H. *et al.* (2010) PARP1 gene knock-out increases resistance to retinal degeneration without affecting retinal function. *PloS One.*, **5**, e15495.

8 Sancho-Pelluz, J., Alavi, M., Sahaboglu, A., Kustermann, S., Farinelli, P., Azadi, S., van Veen, T., Romero, F.J., Paquet-Durand, F. and Ekstrom, P. (2010) Excessive HDAC activation is critical for neurodegeneration in the rd1 mouse. *Cell Death Dis.*, **1**, 1-9.

9 Venkatesh, A., Ma, S., Le, Y.Z., Hall, M.N., Ruegg, M.A. and Punzo, C. (2015) Activated mTORC1 promotes long-term cone survival in retinitis pigmentosa mice. *J. Clin. Invest.*, **125**, 1446-1458.

10 Yang, Y., Mohand-Said, S., Danan, A., Simonutti, M., Fontaine, V., Clerin, E., Picaud, S., Leveillard, T. and Sahel, J.A. (2009) Functional cone rescue by RdCVF protein in a dominant model of retinitis pigmentosa. *Mol. Ther.*, **17**, 787-795.

11 Comitato, A., Di Salvo, M.T., Turchiano, G., Montanari, M., Sakami, S., Palczewski, K. and Marigo, V. (2016) Dominant and recessive mutations in rhodopsin activate different cell death pathways. *Hum. Mol. Genet.*, in press.

12 Egger, G., Liang, G., Aparicio, A. and Jones, P.A. (2004) Epigenetics in human disease and prospects for epigenetic therapy. *Nature*, **429**, 457-463.

13 Chen, B. and Cepko, C.L. (2009) HDAC4 regulates neuronal survival in normal and diseased retinas. *Science*, **323**, 256-259.

14 Peng, G.H. and Chen, S. (2007) Crx activates opsin transcription by recruiting HAT-containing co-activators and promoting histone acetylation. *Hum. Mol. Genet.*, **16**, 2433-2452.

15 Marks, P., Rifkind, R.A., Richon, V.M., Breslow, R., Miller, T. and Kelly, W.K. (2001) Histone deacetylases and cancer: causes and therapies. *Nat. Rev. Cancer*, **1**, 194-202.

16 Haberland, M., Montgomery, R.L. and Olson, E.N. (2009) The many roles of histone deacetylases in development and physiology: implications for disease and therapy. *Nat. Rev. Genet.*, **10**, 32-42.

17 Pfeiffer-Guglielmi, B., Francke, M., Reichenbach, A., Fleckenstein, B., Jung, G. and Hamprecht, B. (2005) Glycogen phosphorylase isozyme pattern in mammalian retinal Muller (glial) cells and in astrocytes of retina and optic nerve. *Glia*, **49**, 84-95.

18 Zhao, L., Zabel, M.K., Wang, X., Ma, W., Shah, P., Fariss, R.N., Qian, H., Parkhurst, C.N., Gan, W.B. and Wong, W.T. (2015) Microglial phagocytosis of living photoreceptors contributes to inherited retinal degeneration. *EMBO Mol. Med.*, **7**, 1179-1197.

19 Kostic, C., Crippa, S.V., Pignat, V., Bemelmans, A.P., Samardzija, M., Grimm, C., Wenzel, A. and Arsenijevic, Y. (2011) Gene therapy regenerates protein expression in cone photoreceptors in Rpe65(R91W/R91W) mice. *PLoS One*, **6**, e16588.

20 Deguchi, A., Soh, J.W., Li, H., Pamukcu, R., Thompson, W.J. and Weinstein, I.B. (2002) Vasodilator-stimulated phosphoprotein (VASP) phosphorylation provides a biomarker for the action of exisulind and related agents that activate protein kinase G. *Mol. Cancer Ther.*, **1**, 803-809.

21 Bolden, J.E., Peart, M.J. and Johnstone, R.W. (2006) Anticancer activities of histone deacetylase inhibitors. *Nat. Rev. Drug Discov.*, **5**, 769-784.

22 Kazantsev, A.G. and Thompson, L.M. (2008) Therapeutic application of histone deacetylase inhibitors for central nervous system disorders. *Nat. Rev. Drug Discov.*, **7**, 854-868.

23 Alsarraf, O., Fan, J., Dahrouj, M., Chou, C.J., Menick, D.R. and Crosson, C.E. (2014) Acetylation: a lysine modification with neuroprotective effects in ischemic retinal degeneration. *Exp. Eye Res.*, **127**, 124-131.

24 Mitton, K.P., Guzman, A.E., Deshpande, M., Byrd, D., DeLooff, C., Mkoyan, K., Zlojutro, P., Wallace, A., Metcalf, B., Laux, K. *et al.* (2014) Different effects of valproic acid on photoreceptor loss in Rd1 and Rd10 retinal degeneration mice. *Mol. Vis.*, **20**, 1527-1544.

25 Kumar, A., Midha, N., Gogia, V., Gupta, S., Sehra, S. and Chohan, A. (2014) Efficacy of oral valproic acid in patients with retinitis pigmentosa. *J. Ocul. Pharmacol. Ther.*, **30**, 580-586.

26 Clemson, C.M., Tzekov, R., Krebs, M., Checchi, J.M., Bigelow, C. and Kaushal, S. (2011) Therapeutic potential of valproic acid for retinitis pigmentosa. *Br. J. Ophthalmol.*, **95**, 89-93.

27 Mulholland, N.M., Soeth, E. and Smith, C.L. (2003) Inhibition of MMTV transcription by HDAC inhibitors occurs independent of changes in chromatin remodeling and increased histone acetylation. *Oncogene*, **22**, 4807-4818.

28 Schaeferhoff, K., Michalakis, S., Tanimoto, N., Fischer, M.D., Becirovic, E., Beck, S.C., Huber, G., Rieger, N., Riess, O., Wissinger, B. *et al.* (2010) Induction of STAT3-related genes in fast degenerating cone photoreceptors of cpfl1 mice. *Cell. Mol. Life Sci.*, **67**, 3173-3186.

29 Yuan, Z.L., Guan, Y.J., Chatterjee, D. and Chin, Y.E. (2005) Stat3 dimerization regulated by reversible acetylation of a single lysine residue. *Science*, **307**, 269-273.

30 Modi, Y.S., Tanchon, C. and Ehlers, J.P. (2015) Comparative safety and tolerability of anti-VEGF therapy in age-related macular degeneration. *Drug Saf.*, **38**, 279-293.

31 Hamlin, R.L. and Altschuld, R.A. (2011) Extrapolation from mouse to man. *Circ. Cardiovasc. Imaging*, **4**, 2-4.

32 Gojo, I., Jiemjit, A., Trepel, J.B., Sparreboom, A., Figg, W.D., Rollins, S., Tidwell, M.L., Greer, J., Chung, E.J., Lee, M.J. *et al.* (2007) Phase 1 and pharmacologic study of MS-275, a histone deacetylase inhibitor, in adults with refractory and relapsed acute leukemias. *Blood*, **109**, 2781-2790.

33 Minucci, S. and Pelicci, P.G. (2006) Histone deacetylase inhibitors and the promise of epigenetic (and more) treatments for cancer. *Nat. Rev. Cancer*, **6**, 38-51.

34 Rich, K.A., Zhan, Y. and Blanks, J.C. (1997) Migration and synaptogenesis of cone photoreceptors in the developing mouse retina. *J. Comp. Neurol.*, **388**, 47-63.

35 Michalakis, S., Geiger, H., Haverkamp, S., Hofmann, F., Gerstner, A. and Biel, M. (2005) Impaired opsin targeting and cone photoreceptor migration in the retina of mice lacking the cyclic nucleotide-gated channel CNGA3. *Invest. Ophthalmol. Vis. Sci.*, **46**, 1516-1524.

36 Yuodelis, C. and Hendrickson, A. (1986) A qualitative and quantitative analysis of the human fovea during development. *Vision Res.*, **26**, 847-855.

37 Tarpey, P., Thomas, S., Sarvananthan, N., Mallya, U., Lisgo, S., Talbot, C.J., Roberts, E.O., Awan, M., Surendran, M., McLean, R.J. *et al.* (2006) Mutations in FRMD7, a newly identified member of the FERM family, cause X-linked idiopathic congenital nystagmus. *Nat .Genet.*, **38**, 1242-1244.

38 McAllister, J.T., Dubis, A.M., Tait, D.M., Ostler, S., Rha, J., Stepien, K.E., Summers, C.G. and Carroll, J. (2010) Arrested development: high-resolution imaging of foveal morphology in albinism. *Vision Res.*, **50**, 810-817.

39 Kohl, S., Zobor, D., Chiang, W.C., Weisschuh, N., Staller, J., Gonzalez Menendez, I., Chang, S., Beck, S.C., Garcia Garrido, M., Sothilingam, V. *et al.* (2015) Mutations in the unfolded protein response regulator ATF6 cause the cone dysfunction disorder achromatopsia. *Nat. Genet.*, **47**, 757-765.

40 Pow, D.V. and Sullivan, R.K. (2007) Nuclear kinesis, neurite sprouting and abnormal axonal projections of cone photoreceptors in the aged and AMD-afflicted human retina. *Exp. Eye Res.*, **84**, 850-857.

41 Palazzo, A., Ackerman, B. and Gundersen, G.G. (2003) Cell biology: Tubulin acetylation and cell motility. *Nature*, **421**, 230.

42 Kwiatkowski, A.V., Rubinson, D.A., Dent, E.W., Edward van Veen, J., Leslie, J.D., Zhang, J., Mebane, L.M., Philippar, U., Pinheiro, E.M., Burds, A.A. *et al.* (2007) Ena/VASP Is Required for neuritogenesis in the developing cortex. *Neuron*, **56**, 441-455.

43 Reinhard, M., Jouvenal, K., Tripier, D. and Walter, U. (1995) Identification, purification, and characterization of a zyxin-related protein that binds the focal adhesion and microfilament protein VASP (vasodilator-stimulated phosphoprotein). *Proc. Natl. Acad. Sci. U S A*, **92**, 7956-7960.

44 Smolenski, A., Bachmann, C., Reinhard, K., Honig-Liedl, P., Jarchau, T., Hoschuetzky, H. and Walter, U. (1998) Analysis and regulation of vasodilator-stimulated phosphoprotein serine 239 phosphorylation in vitro and in intact cells using a phosphospecific monoclonal antibody. *J. Biol. Chem.*, **273**, 20029-20035.

45 Carter-Dawson, L.D. and LaVail, M.M. (1979) Rods and cones in the mouse retina. II. Autoradiographic analysis of cell generation using tritiated thymidine. *J. Comp. Neurol.*, **188**, 263-272.

46 Morgan, J.L., Soto, F., Wong, R.O. and Kerschensteiner, D. (2011) Development of cell type-specific connectivity patterns of converging excitatory axons in the retina. *Neuron*, **71**, 1014-1021.

47 Ma, H., Butler, M.R., Thapa, A., Belcher, J., Yang, F., Baehr, W., Biel, M., Michalakis, S. and Ding, X.Q. (2015) cGMP/Protein Kinase G Signaling Suppresses Inositol 1,4,5-Trisphosphate Receptor Phosphorylation and Promotes Endoplasmic Reticulum Stress in Photoreceptors of Cyclic Nucleotide-gated Channel-deficient Mice. *J. Biol. Chem.*, **290**, 20880-20892.

48 Hao, Y., Xu, N., Box, A.C., Schaefer, L., Kannan, K., Zhang, Y., Florens, L., Seidel, C., Washburn, M.P., Wiegraebe, W. *et al.* (2011) Nuclear cGMP-dependent kinase regulates gene expression

via activity-dependent recruitment of a conserved histone deacetylase complex. *PLoS Genet.*, **7**, e1002065.

49 Chen, B. and Cepko, C.L. (2007) Requirement of histone deacetylase activity for the expression of critical photoreceptor genes. *BMC Dev. Biol.*, **7:78.**, 78.

50 Szel, A., van Veen, T. and Rohlich, P. (1994) Retinal cone differentiation. *Nature*, **370**, 336.

51 Lerea, C.L., Somers, D.E., Hurley, J.B., Klock, I.B. and Bunt-Milam, A.H. (1986) Identification of specific transducin alpha subunits in retinal rod and cone photoreceptors. *Science*, **234**, 77-80.

52 Wolff, B.E., Bearse, M.A., Jr., Schneck, M.E., Dhamdhere, K., Harrison, W.W., Barez, S. and Adams, A.J. (2015) Color vision and neuroretinal function in diabetes. *Doc. Ophthalmol.*, **130**, 131-139.

53 Valdes, J., Trachsel-Moncho, L., Sahaboglu, A., Trifunovic, D., Miranda, M., Ueffing, M., Paquet-Durand, F. and Schmachtenberg, O. (2016) Organotypic retinal explant cultures as in vitro alternative for diabetic retinopathy studies. *ALTEX*, in press.

54 De Vente, J., Steinbusch, H.W. and Schipper, J. (1987) A new approach to immunocytochemistry of 3',5'-cyclic guanosine monophosphate: preparation, specificity, and initial application of a new antiserum against formaldehyde-fixed 3',5'-cyclic guanosine monophosphate. *Neuroscience*, **22**, 361-373.

55 Blanks, J.C. and Johnson, L.V. (1984) Specific binding of peanut lectin to a class of retinal photoreceptor cells. A species comparison. *Invest. Ophthalmol. Vis. Sci.*, **25**, 546-557.

56 del Amo, E.M., Vellonen, K.S., Kidron, H. and Urtti, A. (2015) Intravitreal clearance and volume of distribution of compounds in rabbits: In silico prediction and pharmacokinetic simulations for drug development. *Eur. J. Pharm. Biopharm.*, **95**, 215-226.

Figure legends

Figure 1. HDAC inhibition protects cone photoreceptors *in vitro*. Long term retinal explant cultures from *cpfl1* and wt animals were subjected to 10 nM TSA or control condition from PN14 to PN24. Glyphos staining (green), specific for cone photoreceptors, suggested that few cones survived at PN24 in untreated *cpfl1* explant cultures (A), while TSA treated retinas displayed a clear increase in the numbers of cones (B). TSA treatment showed no adverse effect on wt treated retinas (C, D). The protective effect of TSA on cones is summarized in the bar graph (E). Error bars represent SEM; Scale bars are 20 µm. ONL-outer nuclear layer containing photoreceptors.

Figure 2. HDAC inhibition protects degenerating cones *in vivo.* A single intravitreal injection of 1 nM or 10 nM TSA at PN14 was sufficient to significantly increase the number of *cpfl1* mutant cones in treated compared to sham injected retinas at PN24 (A, B). In addition, cones from treated retinas were positioned mainly in the upper part of the ONL and had visibly longer inner segments (arrows), compared to sham treatment. *In vivo* treatment of wt animals showed no effects on the cone number, cone positioning, or structure (C, D). Quantification of the cone percentage of non-treated, sham treated, and TSA treated (1 nM and 10 nM) *cpfl1* and wt animals is shown in the bar graph (E). Remarkably, the percentage of cones present was similar to wt for both TSA concentrations. Scale bar in a-d is 20 µm. ONL-outer nuclear layer. INL-inner nuclear layer containing interneurons. GCL-ganglion cell layer.

Figure 3. *Cpfl1* cones are protected also at PN30. Cone survival was analyzed in animals which had received a single intravitreal injection at PN14. At PN30 (*i.e.* 16 days post-injection) sham-treated *cpfl1* retina displayed a strong loss of cone-arrestin-labeled cones (green; A). By comparison, the 10nM TSA treatment preserved almost 90% of cones (B), similar to what was observed in age-matched wt (C). The protective effect of TSA on cones is summarized in the bar graph (D). Error bars represent SEM; Scale bars are 20 µm. ONL-outer nuclear layer.

Figure 4. Cone specific opsins and transducin are expressed and correctly positioned in protected cones. In untreated PN24 *cpfl1* retinas, cones were stained with Glyphos (green, A-C, D-F), and colocalized with M-opsin (magenta, G; merged, M), which was localized appropriately in only some of the cone outer segments, mainly in those positioned in the upper parts of the ONL. In the remaining cone cells, M-opsin was also mislocalized in what seemed to be cytoplasm of misplaced cones close to the border with the INL (arrows) and in cone end feet (arrowheads). A similar mislocalization was observed also with antibodies directed against S-opsin (H, N) and transducin (GNAT2; arrows; I, O). After TSA treatment, not only were there more cones, but also M-opsin (J, P), S-opsin (K, Q), as well as GNAT2 (L, R) were correctly localized almost exclusively in outer segments (P-R). Scale bar is 20 µm. ONL-outer nuclear layer.

Figure 5. HDAC inhibition improves cone migration. *cpfl1* retina displayed cone mislocalization, both *in vitro* and *in vivo*, when compared to wt (A-C). At PN24, cone nuclei were scattered throughout the ONL in cultured (A) and *in vivo cpfl1* mutant retinas (B), while in wild-type retinas cones were positioned exclusively in the upper part of the ONL (C). TSA treatment significantly improved cone migration, both in the *in vitro* (D) and *in vivo* (E) treatment paradigms, while no effect was detectable in wt treated retinas (F). For quantification, the cone migration distance was assessed by measuring the distance between the center of cone nuclei from the outer plexiform layer (dashed line), relative to ONL thickness, measured for each individual section of analyzed retinas. The quantifications show a significant improvement of cone migration *in vitro* (G) and *in vivo* (H), with TSA treatment. Scale bars are 20 µm. ONL-outer nuclear layer.

Abbreviations

HDAC histone deacetylase

HAT histone acetyltransferases

TSA Trichostatin A

Cpfl1 cone photoreceptor function loss 1

AMD age-related-macular degeneration

DR diabetic retinopathy

PDE phosphodiesterase

cGMP 3', 5' -cyclic guanosine monophosphate

PKG cGMP-dependent protein kinase

VASP vasodilator-stimulated-protein

GNAT2 cone specific transducin

wt wild-type

PFA paraformaldehyde

PBS phosphate saline buffer

TUNEL terminal deoxynucleotidyl transferase dUTP nick end labeling

ONL outer nuclear layer

OPL outer plexiform layer

IS inner segment

DAPI 4',6-diamidino-2-phenylindole

PN postnatal

Glyphos Glycogen phosphorylase

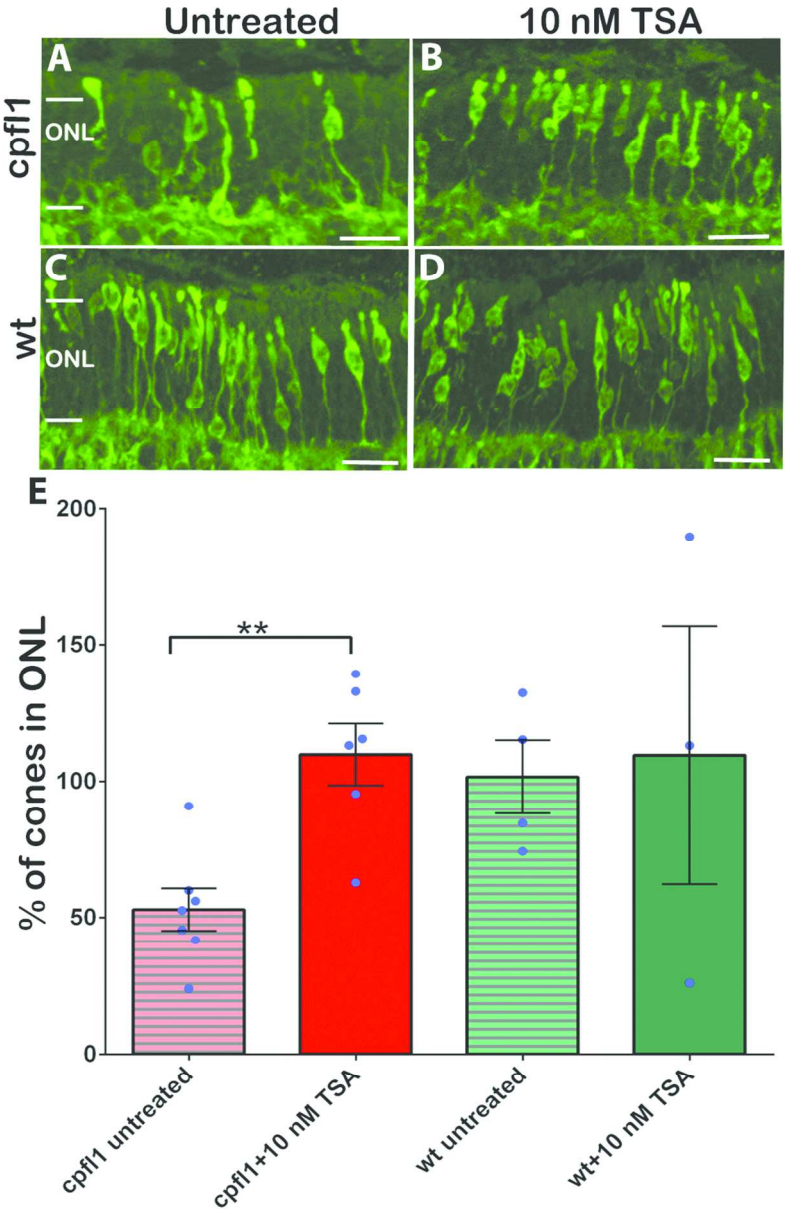

HDAC inhibition protects cone photoreceptors in vitro.

84x129mm (300 x 300 DPI)

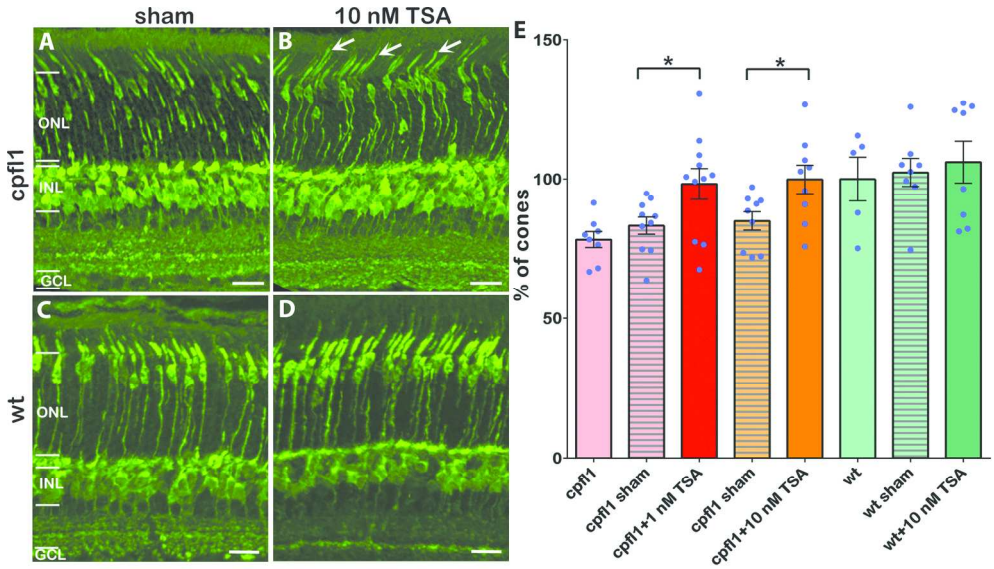

HDAC inhibition protects degenerating cones in vivo.

169x95mm (300 x 300 DPI)

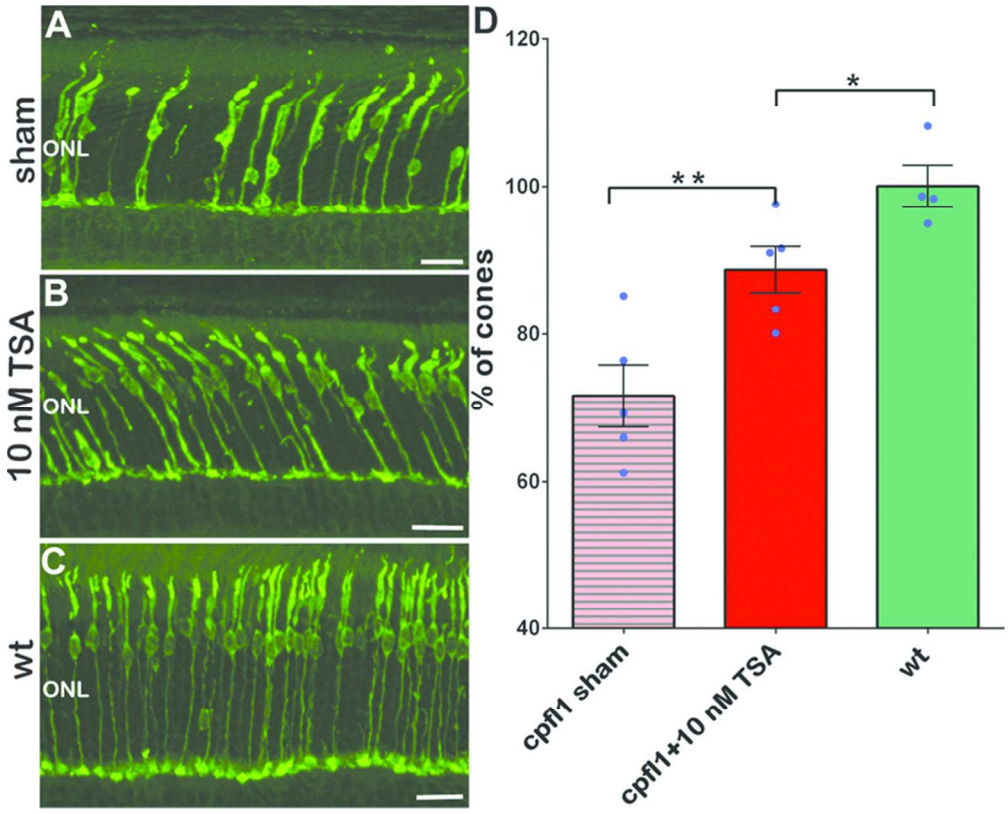

Cpfl1 cones are protected also at PN30.

69x55mm (300 x 300 DPI)

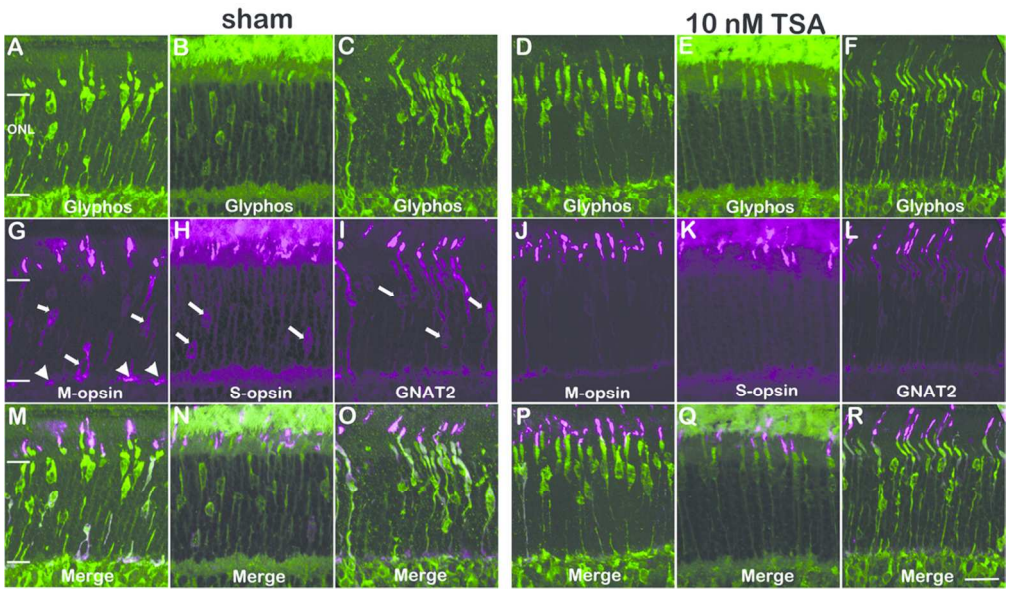

Cone specific opsins and transducin are expressed and correctly positioned in protected cones.

101x59mm (300 x 300 DPI)

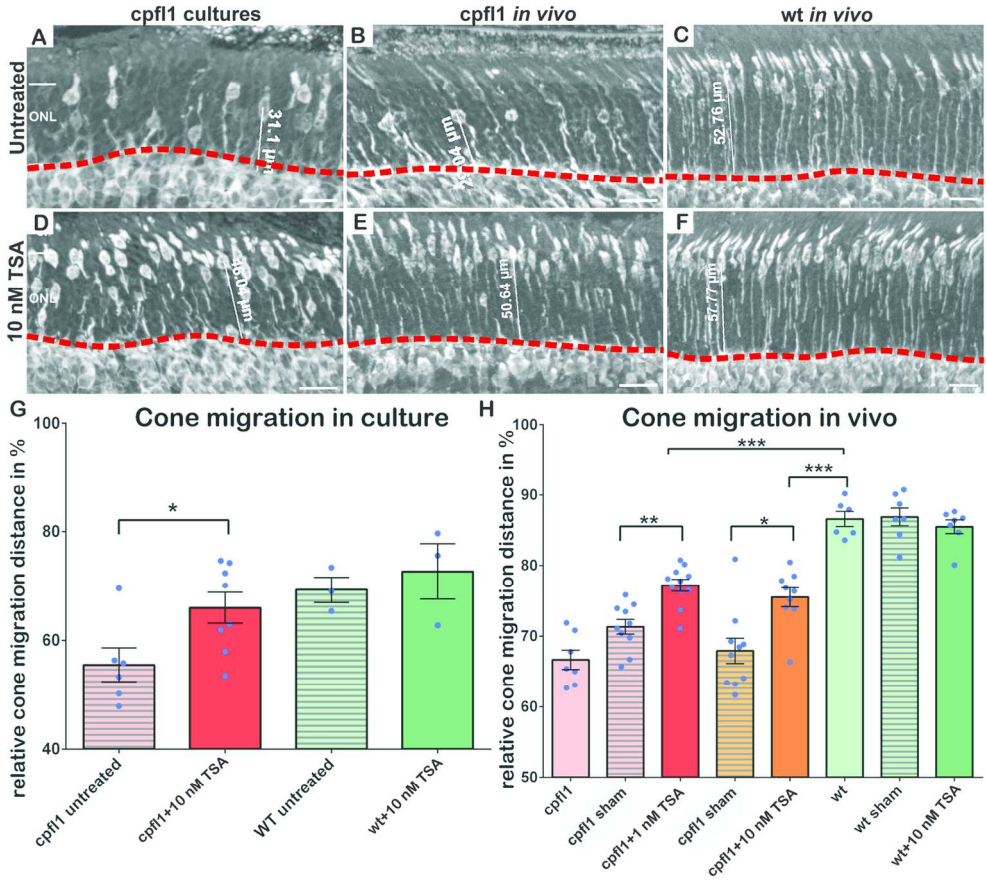

HDAC inhibition improves cone migration.

154x137mm (300 x 300 DPI)